Pulsed-light soaking of hydrogenated amorphous silicon

M. Stutzmann,* M. C. Rossi, and M. S. Brandt*

Max-Planck-Institut für Festkörperforschung, Heisenbergstrasse 1, D-70569 Stuttgart, Germany

(Received 14 March 1994)

We investigate in detail the creation of metastable dangling bond defects in undoped hydrogenated amorphous silicon by illumination with pulsed-light sources. Based on the electron-hole recombination model for defect creation, the kinetics of the defect generation process is analyzed theoretically for different experimental conditions (pulse length, pulse energy, repetition rate, and average intensity). These theoretical results are then compared to experimental observations using both monochromatic and polychromatic ("white light") pulse sources. Implications of pulse illumination for accelerated testing of the stability of amorphous-silicon-based solar cells are also discussed.

I. INTRODUCTION

Recently, two alternative illumination schemes to study the light-induced degradation of amorphous silicon have been introduced. The first of these is the constant degradation method (CDM). This technique uses a continuously adjusted light intensity to keep the photocurrent during degradation constant, resulting in a considerable simplification (linearization) of the defect creation kinetics.[1] In this paper, we will discuss in detail the second alternative approach, namely, the use of pulsed-light sources for the degradation of a-Si:H. We first outline the theory of metastable defect creation by pulse illumination in the context of weak-bond breaking, and then present experimental details, in particular concerning pulsed light sources with different pulse lengths and peak intensities. Experimental results are presented in two sections: the first describes experiments performed using homogeneously absorbed monochromatic laser light, whereas the second section discusses the use of white light from a high-power Xe flash lamp useful to simulate the degradation behavior under conditions similar to natural AM1.5 sun light. A brief description of several aspects discussed in detail here have already been described in previous publications.[2-4] Especially, possible applications of pulsed light soaking for accelerated stability testing of a-Si:H solar cells have been discussed in Ref. 4.

II. THEORY OF METASTABLE DEFECT CREATION BY LIGHT PULSES

We begin our discussion by recalling Eq. (3) of Ref. 2, which describes the dependence of the generalized carrier densities $\tilde{n}$ and $\tilde{p}$ on the normalized defect density, $\tilde{N}$, and generation rate, $\tilde{G}$:

$$\tilde{n} = \frac{\tilde{G}}{\frac{\tilde{N}}{2} + \left[\left(\frac{\tilde{N}}{2}\right)^2 + \tilde{G}\right]^{1/2}} \, . \tag{1a}$$

An equivalent way of writing this equation is

$$\tilde{n} = \left[\left(\frac{\tilde{N}}{2}\right)^2 + \tilde{G}\right]^{1/2} - \frac{\tilde{N}}{2} \, . \tag{1b}$$

The basic assumption leading to these relations is that carrier recombination occurs either by direct tail-to-tail recombination (bimolecular limit, $\tilde{n} \propto \sqrt{\tilde{G}}$) or, at sufficient high defect densities, via those defect states acting as recombination centers (monomolecular limit, $\tilde{n} = \tilde{G}/\tilde{N}$). Equation (1b) is then obtained by solving the coupled rate equations for $\tilde{n}$ and $\tilde{p}$ in the steady state

$$\frac{d\tilde{n}}{dt} = \tilde{G} - \tilde{n}\tilde{N} - \tilde{n}\tilde{p} = 0 \quad , \quad \frac{d\tilde{p}}{dt} = \tilde{G} - \tilde{p}\tilde{N} - \tilde{n}\tilde{p} = 0 \, . \tag{2}$$

In Fig. 1, we show the dependence of $\tilde{n}$ on $\tilde{G}$ for various defect densities, $\tilde{N}$, according to Eq. (1). One clearly recognizes the monomolecular limit for low $\tilde{G}$ and large $\tilde{N}$, and the bimolecular limit for low $\tilde{N}$ and high $\tilde{G}$, respectively. The quantity γ indicated in Fig. 1 is the exponent in the relation $\tilde{n} = \tilde{G}^\gamma$, i.e., it describes the dependence of the photoconductivity on light intensity in amorphous silicon for a constant defect density. The dependence of γ on $\tilde{G}$ and $\tilde{N}$ can also be obtained from Eq. (1) and is plotted in Fig. 2. For a constant generation rate, $\tilde{G}$, the transition from $\gamma = 1/2$ (bimolecular recombination) to $\gamma = 1$ (monomolecular recombination) occurs completely when $\tilde{N}$ increases by approximately two orders of magnitude. For a fixed defect density, $\tilde{N}$, on the other hand, the same transition requires approximately four orders of magnitude changes in $\tilde{G}$.

Since an understanding of the recombination in a-Si:H over many orders of magnitude in generation rate under simultaneously varying defect densities is necessary for a quantitative modeling of pulse-light degradation, we have first tested the applicability of Eq. (1b) for conventional illumination with cw light, determining simultaneously $\tilde{n}(\propto \sigma_{ph})$, γ, and $\tilde{N}$ ($\propto N_S$, spin density). In
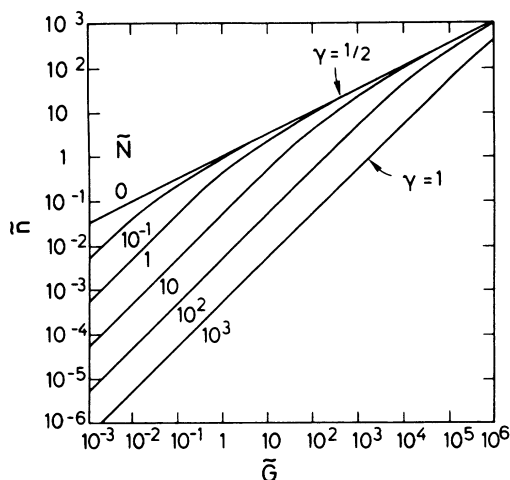
FIG. 1. Dependence of the generalized free carrier density $\tilde{n}$, on the generalized generation rate, $\tilde{G}$, for different defect densities, $\tilde{N}$, according to Eq. (1). $\gamma = \frac{1}{2}$ ($\gamma = 1$) represents the bimolecular (monomolecular) limit of the underlying recombination process.

FIG. 3. Experimental results for the dependence of the room-temperature photoconductivity in undoped a-Si:H on the illumination intensity (monochromatic light, $\hbar\omega = 1.92$ eV). States A and B refer to the annealed condition and results after light soaking, respectively.

the annealed state, "A," of a-Si:H with a defect density of $\approx 5 \times 10^{15}$ cm^{-3}, the bimolecular to monomolecular transition at 300 K occurs around light intensities of 10 mW/cm^2 for homogeneously absorbed light. This is shown by the open symbols in Fig. 3. After long exposure to intense cw light the defect density in the sample has increased to more than 10^{17} cm^{-3} (state "B") and, as demonstrated by the solid symbols in Fig. 3, the photoconductivity is now essentially monomolecular (i.e., $\gamma \approx 1$, $\sigma_{\text{ph}} \propto I$) over the entire range of light intensities shown in Fig. 3. Details of the transition from state "A" to "B" are shown in Fig. 4, where we compare the dependence of the photoconductivity, the inverse spin density, N_S^{-1}, and of the exponent γ on illumination time, t_{ill}. In the case of Figs. 3 and 4, illumination was performed at room temperature with monochromatic laser light of a wavelength (647 nm) sufficiently large so that for a sample of ≈ 1 μm the light is absorbed in an approximately homogeneous fashion. This experimental precaution is a prerequisite for a kinetic behavior of σ_{ph}, γ, and N_S which can be treated in a simple single layer model. Since
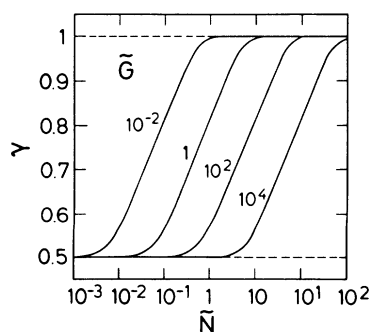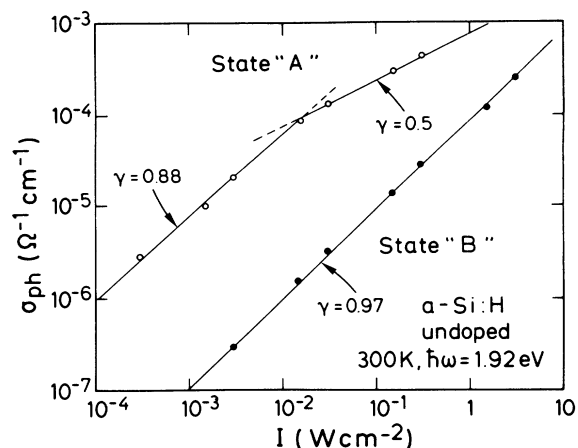
the changes observed in Fig. 4 are highly nonlinear in illumination time and/or intensity, strongly inhomogeneous illumination conditions would require more complicated multilayer models in order to correctly describe macroscopic quantities such as the photoconductivity or the spin density.

For homogeneous illumination conditions, we have previously derived kinetic equations for the photoconductivity and the ESR spin density based on the assumption that new metastable defects are created by a bimolecular nonradiative recombination event between excited electrons and holes trapped in tail states.[5] The resulting
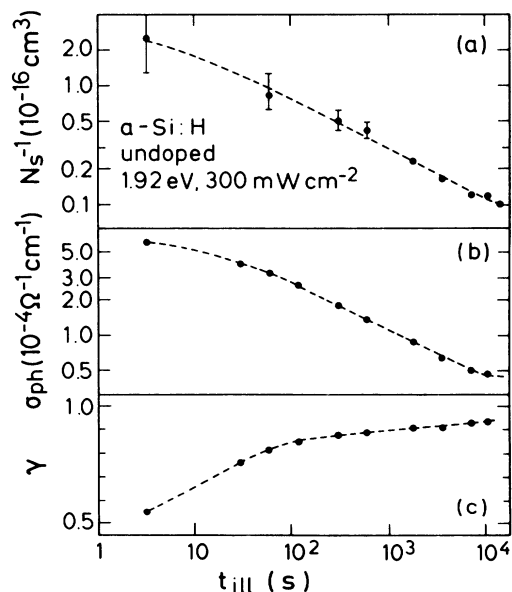

FIG. 2. Dependence of the exponent γ ($\tilde{n} \propto \tilde{G}^{\gamma}$) for different generation rates $\tilde{G}$ on the generalized defect density, $\tilde{N}$.

FIG. 4. Inverse ESR-spin density [N_S^{-1}, (a)], photoconductivity [τ_{ph}, (b)], and exponent γ (c) as a function of illumination time during a typical cw-light-soaking experiment of undoped a-Si:H.

defect creation rate,

$$\frac{dN}{dt} = c_{sw}np \qquad (3)$$

is then solved self-consistently with Eq. (1) under the condition that the generation rate, G, of electrons and holes is kept constant during the experiment (i.e., constant light intensity). The resulting exact solution for σ_{ph} and N_S as a function of illumination time is somewhat complicated. A simplification results if the defect density, N, is already sufficiently large so that the recombination of photoexcited carriers occurs almost entirely via these defects, without a significant contribution of tail-to-tail recombination. Then we expect from Eq. (1) $\tilde{n} \approx \tilde{G}/\tilde{N}$, and a similar dependence for $\tilde{p}$. Putting this approximation back into Eq. (3), one easily obtains as a long-time limit:

$$\sigma_{ph} \propto \frac{G}{N_S} \quad \text{(e.g., } \gamma = 1\text{)} \qquad (4a)$$

and

$$N(t_{ill}) \propto t_{ill}^{1/3}. \qquad (4b)$$

As demonstrated by the experimental results in Fig. 4, Eqs. (4a) and (4b) are indeed a good approximation for the long-time behavior during cw light soaking of undoped a-Si:H. $\gamma \approx 1$ is fulfilled after several hundred seconds of illumination with an intensity of 300 mW/cm^2. Once this transition to monomolecular photoconductivity has occurred, one observes $N_S \propto t_{ill}^{1/3}$ and $\sigma_{ph} \propto N_S^{-1}$, as expected from Eq. (4).

Comparing the experimental results summarized in Figs. 3 and 4, we find that Eqs. (1) and (4) provide a reasonable quantitative description of the light-soaking process using cw illumination at temperatures around 300 K. In terms of the generalized quantities $\tilde{n}$, $\tilde{G}$, and $\tilde{N}$ in Eq. (1) and Fig. 1, the experimental situation of a-Si:H in the annealed state, "A" (i.e., $N_S = 5 \times 10^{15}$ cm^{-3}) under illumination with 100 mW/cm^2 homogeneously absorbed light corresponds to $\tilde{N} = 1$, $\tilde{G} = 1$, and $\tilde{n} = 0.3$. Light soaking increases $\tilde{N}$ to about 30 with corresponding decrease of $\tilde{n}$ to about 10^{-2}. In this state "B," the photoconductivity remains essentially monomolecular up to light intensities of about 10 W/cm^2 or more ($\tilde{G} \approx 100$ in Fig. 1). However, for such high cw illumination intensities, heating of the sample by the absorbed light becomes a major problem. This point has been discussed in detail in a preceding paper.[1] A deviation of the sample temperature from 300 K by more than 20 or 30 K will give rise to significant changes of the recombination processes in a-Si:H and also affect the long-time behavior of the metastable defect creation due to simultaneous defect annealing.[5]

A second situation in which Eq. (4b) will lose its validity is the existence of a true saturation value for the metastable defect density because of the exhaustion of available defect creation sites (impurities or other special bonding configurations). Such a scenario has been proposed by other groups based on their analysis of the defect creation kinetics.[6–8] Values for the saturated de-

fect density in a-Si:H as cited by these groups are about 2×10^{17} cm^{-3}. It will be one purpose of this paper to show that larger defect densities can be realized easily by the use of pulse illumination.

Having described the case of cw illumination on the basis of Eqs. (1) and (4), we now turn to the discussion of pulse illumination. For the sake of simplicity, we shall assume that the light pulses have a rectangular shape with a pulse duration t_p. This is a reasonable approximation for $t_p \ll \tau$ and also for $t_p \gg \tau$, where τ is the characteristic decay time of photoconductivity in a-Si:H at room temperature ($\tau \approx 1$ μsec). In addition to the light-pulse duration, the pulse repetition rate, ν_{rep}, and the average light-intensity, $\langle I \rangle$, are required for a characterization of the pulse-illumination conditions. In terms of these quantities we can then calculate other important quantities such as (i) the illumination duty cycle, $\eta = t_p\nu_{rep}$; (ii) the light intensity during the pulse, $I_p = \langle I \rangle /\eta$; (iii) the individual pulse energy density, $E_p = I_p t_p = \langle I \rangle /\nu_{rep}$. A condition which should be fulfilled in all cases of pulse irradiation is $1/\nu_{rep} \gg \tau$, i.e., the time between pulses should be sufficiently long to allow a complete relaxation and recombination of excited carriers in order to avoid pileup effects. Thus, the optimal repetition rate in a-Si:H with $\tau \approx 10^{-6}$ s is about 10 kHz for submicrosecond pulses, corresponding to a maximum value of $\eta \approx 10\%$.

A second important quantity is the individual pulse energy density, E_p. During and following a pulse, optically excited carriers thermalize and recombine, transforming all electronic energy eventually into thermal energy. Since the electronic relaxation times ($< 10^{-6}$ s) are much shorter than thermal relaxation times for a-Si:H on an insulating substrate ($\approx 10^{-3}$ s), a given pulse energy causes a temperature rise in the amorphous silicon film which can be estimated to

$$\Delta T \approx E_p A/c_p V = E_p/c_p d . \qquad (5)$$

Here, V, A, and d are the volume, area, and thickness of the a-Si:H sample, respectively, and c_p is the heat capacity of a-Si:H per unit volume ($c_p \approx 2$ J cm^{-3} K^{-1}). Thus for a typical sample with dimensions 1 cm $\times$ 1 cm $\times$ 1 μm, a pulse energy density of $E_p = 10^{-3}$ J/cm^2 translates into a temperature rise of $\Delta T \approx 5$ K. (For comparison, note that the threshold for recrystallization of thin a-Si:H layers by single laser pulses occurs at pulse energy densities of ≈ 100 mJ/cm^2.) Therefore, in order to avoid thermal effects which might influence the observed metastable defect creation, single pulse energy densities should not exceed 10 mJ/cm^2, a limit which obviously depends to some extent on the actual pulse duration employed and on the absorption depth. In the experiments described here, pulse energy densities were typically below 1 mJ/cm^2, so that unwanted thermal effects can be excluded.

For our discussion of metastable defect creation by pulse illumination we start again from Eq. (3), this time integrating over each pulse separately. The discrete increase in defect density per pulse, ΔN, is then given by

$$\Delta N = \int_{t_{\min}}^{1/\nu_{\rm rep}} c_{\rm sw} n p \, dt \approx c_{\rm sw} \int_{10^{-12}s}^{10^{-5}s} n^2(t) dt \qquad (6)$$

where $t_{\min}$ is a short-time limit for defect creation following from the fact that some motion of network atoms is necessary for creating metastable defect sites ($t_{\min} \geq 10^{-12}$ s), and the long-time limit of the integral in Eq. (6) is given by the inverse repetition rate or the excess carrier lifetime, whichever is shorter. Obviously, our knowledge of recombination processes in a-Si:H is not sufficient to accurately model the seven orders of magnitude in time spanned by the integration limits of Eq. (6). Instead, we divide the carrier thermalization and recombination process into three regimes.

(i) The initial femtosecond and picosecond time regime, in which carriers thermalize into the band tail states and partly recombine via Auger processes. This regime will not contribute significantly to the integral in Eq. (6) because of the short time scale. In addition, unthermalized carriers can be expected to have a smaller probability for defect creation than carriers localized in tail states because of their smaller electron-phonon interaction. We also like to mention that for the pulsed-light sources used in the experiments described below the individual pulse energy density was typically of the order of $10^{-5} - 10^{-4}$ J cm^{-2}, corresponding to a density of generated electron-hole pairs of $\approx 3 \times 10^{17} - 3 \times 10^{18}$ cm^{-3} for a 1 μm thick film. For such a density, Auger recombination is not yet very likely, so that not much recombination occurs in this time range.

(ii) In the time range extending from nanoseconds to microseconds, all photoexcited carriers will have relaxed into the band tails and can recombine by bimolecular recombination. Deep trapping and nonradiative recombination at dangling bonds will not take place yet. For a purely bimolecular recombination, $n(t) \approx p(t)$ in Eq. (6) is independent of the existing defect density, N:

$$\frac{dn}{dt} = -anp = -an^2 , \qquad (7a)$$

$$\frac{1}{n(t)} - \frac{1}{n(0)} = at . \qquad (7b)$$

Inserting Eq. (7a) into Eq. (6), we obtain immediately

$$\Delta N = -c_{\rm sw} \int_0^\infty \frac{1}{a} \frac{dn}{dt} dt = \frac{c_{\rm sw}}{a} n(0), \qquad (8)$$

which means that the increase in defect density per pulse in this regime is simply proportional to the initial excess carrier density, $n(0)$, i.e., to the pulse energy density, E_p. From Eq. (8), we obtain easily the increase of the defect density with illumination time (using $dN/dt = \Delta N \nu_{\rm rep}$):

$$N(t_{\rm ill}) = N(0) + \Delta N \nu_{\rm rep} t_{\rm ill} = N(0) + \frac{c_{\rm sw}}{a} n(0) \nu_{\rm rep} t_{\rm ill} . \qquad (9)$$

Since $n(0) \propto E_p = \langle I \rangle / \nu_{\rm rep}$, Eq. (9) shows that for purely bimolecular recombination, the defect density increases linearly with exposure time and average light intensity.

We note in passing that a relation similar to Eq. (9) is

observed in the case of metastable defect creation in a-Si:H by irradiation with ionizing particles.[9,10] As a matter of fact, it is possible to view particle bombardment as an extreme case of pulse irradiation, where a large number of electron-hole pairs are generated in a small volume close to the particle trajectory [e.g., $\approx 10^4$ electron-hole pairs per μm$^{-3}(10^{16}$ cm$^{-3})$ for 20 keV electrons]. Since the local excess carrier density is comparable to or larger than the defect density, it is likely that a considerable fraction of the recombination traffic occurs bimolecularly.

(iii) The third time regime to be considered is the one corresponding to the typical time constant, τ, of recombination at deep defects. In a-Si:H at 300 K, τ is determined by the trapping of excess electrons at neutral dangling bonds:

$$\frac{dn}{dt} = -bnN = -\frac{n}{\tau}, \quad \tau = \frac{1}{bN} . \qquad (10a)$$

The solution of Eq. (10a) obviously is an exponential decay:

$$n(t) = n(0) \exp\left(-\frac{t}{\tau}\right) . \qquad (10b)$$

For a defect density of $N = 10^{16}$ cm^{-3}, a typical value for τ is $\tau \approx 10^{-6}$ s, i.e., $b \approx 10^{-10}$ cm^3/s. Inserting Eq. (10b) into Eq. (6) we obtain in the case of monomolecular recombination:

$$\Delta N = \frac{1}{2} c_{\rm sw} n^2(0)\tau = \frac{1}{2} c_{\rm sw} n^2(0)\frac{1}{bN} . \qquad (11)$$

Contrary to the bimolecular recombination, in the case of Eq. (11) ΔN depends on N, and an integration over sequential pulses yields

$$N^2(t_{\rm ill}) = N^2(0) + \frac{c_{\rm sw}}{b} n^2(0)\nu_{\rm rep} t_{\rm ill} . \qquad (12)$$

Again, the pulse energy density, the initial carrier density and the average power density are related by $E_p = \langle I \rangle / \nu_{\rm rep} \propto n(0)$, so that for long illumination times Eq. (12) can be approximated by

$$N(t_{\rm ill}) \propto \left(\frac{c_{\rm sw}}{b\nu_{\rm rep}}\right)^{1/2} \langle I \rangle t_{\rm ill}^{1/2} . \qquad (13)$$

Thus, in the monomolecular limit, the metastable defect density should increase proportional to the average generation rate and as the square root of illumination time.

For a more general description of metastable defect creation by pulse illumination with $t_p \ll \tau$, we have to take into account that during carrier relaxation following an intense pulse initially bimolecular recombination will dominate, eventually crossing over into monomolecular recombination as time goes on. In the context of Fig. 1, the problem is to quantitatively describe trajectories in the $\tilde{n}$-versus-$\tilde{G}$ diagram which always start on the bimolecular limit ($\tilde{N} = 0$), but branch into curves for increasing $\tilde{N}$ as pulse-illumination proceeds. In this case, carrier recombination after pulse excitation will be given by a superposition of the bimolecular [Eq. (7)] and

M. STUTZMANN, M. C. ROSSI, AND M. S. BRANDT

the monomolecular limits [Eq. (10)] according to

$$\frac{dn}{dt} = -an^2 - bnN \ . \tag{14a}$$

Integration of this equation yields

$$n(t) = n(0)\frac{bN}{bN + an(0)}\frac{\exp\left[-bNt\right]}{1 - \frac{an(0)}{bN+an(0)}\exp\left[-bNt\right]} \ , \tag{14b}$$

where again $bN = 1/\tau$ defines the monomolecular lifetime of carriers due to recombination at dangling bonds. The long-time limit of Eq. (14b) is given by

$$n(t) \to n(0)\frac{bN}{bN + an(0)}\exp\left(-bNt\right) \ , \tag{14c}$$

which constitutes the same exponential decay as in Eq. (10b), however, with a prefactor depending on the branching of the excess carrier decay into the monomolecular (bN) or bimolecular $(an(0))$ recombination channel.

Combining Eq. (6) with Eqs. (14a) and (14b) we obtain for the defect density increase per pulse

$$\Delta N = c_{\rm sw}\int_0^\infty n^2(t)dt$$

$$= -\frac{c_{\rm sw}}{a}\left\{\int_0^\infty \frac{dn}{dt}dt + bN\int_0^\infty n(t)dt\right\} \ , \tag{15}$$

with the solution

$$\Delta N = \frac{c_{\rm sw}}{a}n(0)\left\{1 - \frac{bN}{an(0)}\ln\left(1 + \frac{an(0)}{bN}\right)\right\} \ . \tag{16}$$

Note that for $an(0) \gg bN$, this equation transforms into Eq. (8) for the purely bimolecular case, whereas for $an(0) < bN$ expansion of $\ln[1 + an(0)/bN]$ into a Taylor series $[\ln(1 + x) \approx x - \frac{1}{2}x^2$ for $x < 1]$ reproduces the monomolecular limit, Eq. (11).

In order to see which limiting case should be applied to pulse degradation of a-Si:H at room temperature, we need estimates for the parameters a, b, N, and $n(0)$ in Eq. (16). Here, N and $n(0)$ can be either measured directly or are determined by the pulse-light sources employed. Typical values are $N \approx 10^{17} - 10^{18}$ cm^{-3} for long-pulse illumination, and $n(0) \approx 10^{18}$ cm^{-3} using the short-pulse laser sources described below. The ratio a/b can be estimated from the transition between monomolecular and bimolecular recombination for a-Si:H as described above (cf. Figs. 1–4). As a rough estimate, we obtain $a/b \approx 3$, leading to two approximate solutions. In the initial phases of pulse degradation, the defect density is so low $(N \approx 10^{16}$ cm$^{-3})$ that bimolecular recombination dominates [Eqs. (8) and (9)]. For defect densities above 10^{19} cm^{-3}, on the other hand, even for pulse illumination the monomolecular limit, Eqs. (11) and (12), prevails. This is shown in more detail in Fig. 5, where the expression on the right-hand side of Eq. (16) is shown as a function of $x = an(0)/bN$. For small N one finds in Eq. (16) $\{\ \} \approx 1$, whereas for large $N\{\ \} \propto 1/N$. Unfortunately, neither of these two simple limits applies to state-of-the-art a-Si:H, where the long-time behavior
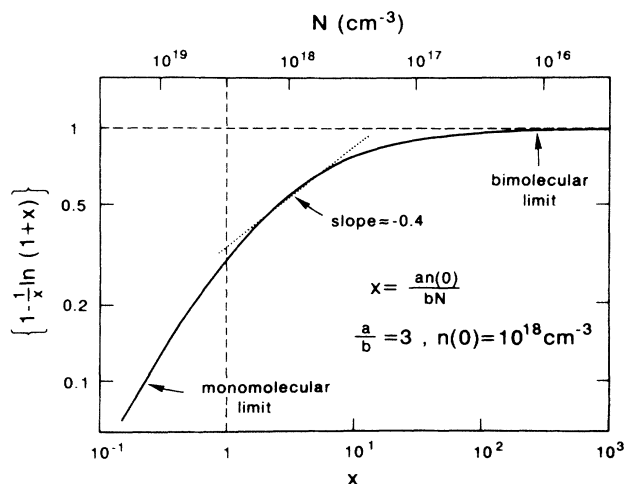

FIG. 5. Graphical representation of the term $1 - \frac{1}{x}\ln(1+x)$ in Eq. (16) as a function of x.

during pulse soaking is characterized by defect densities in the range $3 \times 10^{17} - 2 \times 10^{18}$ cm^{-3}. Since Eq. (16) cannot be solved analytically, we use an approximation indicated by the dotted line in Fig. 5, namely,

$$\Delta N \approx \frac{\tilde{c}_{\rm sw}}{a}n(0)N^{-\delta} \ , \tag{17}$$

where $\delta \approx 0.4$, and in addition $\tilde{c}_{\rm sw}$ now depends weakly on $n(0)$. Integration of Eq. (17) yields

$$N^{1+\delta}(t_{\rm ill}) = N^{1+\delta}(0) + (1 + \delta)\frac{\tilde{c}_{\rm sw}}{a}n(0)t_{\rm ill} \ . \tag{18}$$

In the long-time limit this approaches a time dependence of $t_{\rm ill}^{0.7}$, i.e., intermediate between the linear dependence of the bimolecular limit, Eq. (9), and the square-root dependence of the monomolecular limit, Eq. (13).

The theory of pulsed light soaking as discussed so far was based on Eq. (6) together with the assumption of very short pulses, $t_p \ll \tau$. A second case which can occur is that of a pulse duration long compared to the carrier recombination time, $t_p \gg \tau$. In the latter case, the carrier concentration reaches a steady state during each pulse, which will be given by the solution of the rate equations $(G_p \propto I_p$ is the generation rate during the light pulse):

$$0 = \frac{dn}{dt} = G_p - anp - bnN \ ,$$

$$0 = \frac{dp}{dt} = G_p - anp - bpN \ , \tag{19}$$

where as before we assume for the sake of simplicity that the transition probability b for recombination via a defect is the same for electrons and holes.[12] The solution of Eq. (19) is given by Eq. (1b), now including specific transition probabilities:

$$n = p = \left[\left(\frac{bN}{2a}\right)^2 + \frac{G_p}{a}\right]^{1/2} - \frac{bN}{2a} \ . \tag{20}$$

For the metastable defect creation, according to Eq. (3) we obtain for the increase in defect density per pulse

$$\Delta N = c_{\mathrm{sw}} \int_0^{t_p} n^2 dt = c_{\mathrm{sw}} n^2 \left(G_p, N\right) t_p \ , \qquad (21)$$

where, contrary to Eq. (6) for short pulses, n^2 is now assumed to be constant during a given pulse:

$$n^2 = \frac{bN}{a} \left(\frac{bN}{2a} - \left[\left(\frac{bN}{2a}\right)^2 + \frac{G_p}{a} \right]^{1/2} \right) + \frac{G_p}{a} \ . \quad (22\mathrm{a})$$

For the integration of Eq. (21) it is more convenient to use an equivalent expression for n^2, namely,

$$n^2 = G_p^2 \left\{ \frac{bN}{2} + \left[\left(\frac{bN}{2}\right)^2 + aG_p \right]^{1/2} \right\}^{-2} \ . \quad (22\mathrm{b})$$

Inserting Eq. (22b) into Eq. (21), we finally obtain

$$\left\{ \frac{bN}{2} + \left[\left(\frac{bN}{2}\right)^2 + aG_p \right]^{1/2} \right\}^2 dN = c_{\mathrm{sw}} G_p^2 \nu_{\mathrm{rep}} t_p dt_{\mathrm{ill}}. $$

$$(23)$$

Equation (23) is formally equivalent to Eq. (11) of Ref. 5, where the case of continuous illumination was discussed. Except for a change of notation $(a \leftrightarrow A_t, \ b \leftrightarrow A_n = A_p, \ c_{\mathrm{sw}} \leftrightarrow c_{\mathrm{sw}} A_t)$, the physically relevant difference between Eq. (23) here and Eq. (11) of Ref. 5 is the replacement of the average generation rate $\langle G \rangle$ by G_p, the generation rate during the pulse, and the appearance of an additional factor $\nu_{\mathrm{rep}} t_p = \eta$ (duty cycle) on the right-hand side of Eq. (23). Before writing down the complex solution of Eq. (23) which will provide the general kinetic behavior of $N(t)$ in the case of illumination with long light pulses, we briefly discuss the monomolecular and the bimolecular limits of Eq. (23). This will provide a simple physical picture of how defect generation in a-Si:H can be accelerated by pulsed illumination. For the bimolecular limit, $\left(\frac{bN}{2}\right)^2 \ll aG_p$, we obtain from Eq. (23)

$$dN = \frac{c_{\mathrm{sw}}}{a} G_p \nu_{\mathrm{rep}} t_p dt_{\mathrm{ill}} = \frac{c_{\mathrm{sw}}}{a} \langle G \rangle dt_{\mathrm{ill}} \ , \quad (24)$$

where we have used the relation $\langle G \rangle = G_p \nu_{\mathrm{rep}} t_p$. Thus, in the bimolecular limit, N increases linearly with illumination time and *average* light intensity, so that there is *no difference between continuous and pulsed illumination as long as bimolecular recombination dominates*. In particular, we recover from Eq. (24) the case of Eq. (9) (bimolecular limit of very short pulses) by noting that $n(0)\nu_{\mathrm{rep}} \propto \langle G \rangle$. As a consequence, the initial degradation behavior of device grade a-Si:H, which is always dominated by bimolecular recombination (cf. Fig. 3) for intensities larger than ≈ 10 mW cm^{-2}, should be independent of the time distribution of incoming photons. Physically, this is a simple consequence of the creation of metastable defects by tail-to-tail recombination, Eq.

(3). The defects, ΔN, created per unit time are proportional to $\langle n^2 \rangle$, which in turn is proportional to $\langle I \rangle$ in the bimolecular case, $n \propto I^{1/2}$.

A change in kinetics only occurs when monomolecular recombination via (stable and metastable) defects becomes more and more important as time goes by. The monomolecular limit, $\left(\frac{bN}{2}\right)^2 \gg aG_p$, of Eq. (23) is given by

$$dN = \frac{c_{\mathrm{sw}}}{b^2} \frac{G_p^2}{N^2} \nu_{\mathrm{rep}} t_p dt_{\mathrm{ill}} = \frac{c_{\mathrm{sw}}}{b^2} \frac{\langle G \rangle^2}{N^2} \frac{1}{\eta} dt_{\mathrm{ill}} \ , \quad (25)$$

where $\eta = \nu_{\mathrm{rep}} t_p$ is the illumination duty cycle. From Eq. (25) we find easily that for the same average light intensity, $\langle G \rangle$, pulsed illumination with long light pulses enhances the defect creation rate by $\frac{1}{\eta} \gg 1$, but does not change the analytical dependence of N on $\langle G \rangle$ and t_{ill}:

$$N^3(t_{\mathrm{ill}}) - N^3(0) = \frac{3c_{\mathrm{sw}}}{b^2} \frac{1}{\eta} \langle G \rangle^2 t_{\mathrm{ill}} \ . \quad (26)$$

Since in the derivation of Eq. (26) we have assumed $t_p > \tau$, the largest enhancement of the defect creation rate should be obtained in a-Si:H by pulses with a duration of several μsec with a low repetition rate. The physical origin of the enhancement in defect creation rate in the monomolecular limit is also easy to see: With $n \propto G$ we have $\langle n^2 \rangle \propto \langle G^2 \rangle \gg \langle G \rangle^2$ when photons are bunched in short intense pulses rather than being provided at a low continuous rate.

We finish our derivation of the defect creation kinetics in a-Si:H by pulse illumination by writing down the explicit solution of Eq. (21) as the general kinetic equation for long light pulses. The solution in this case is similar to Eq. (12) of Ref. 5:

$$\left[N^3(t_{\mathrm{ill}}) - N^3(0)\right] + \left(\frac{2}{b}\right)^3 \left\{ \left[\left(\frac{b}{2}N(t_{\mathrm{ill}})\right)^2 + aG_p \right]^{3/2} \right.$$
$$\left. - \left[\left(\frac{b}{2}N(0)\right)^2 + aG_p \right]^{3/2} \right\}$$

$$+6\frac{a}{b^2} G_p \left[N(t_{\mathrm{ill}}) - N(0)\right] = 6\frac{c_{\mathrm{sw}}}{b^2} G_p^2 \nu_{\mathrm{rep}} t_p t_{\mathrm{ill}} \ . \quad (27)$$

We shall now turn to the description of pulse-illumination experiments using different light sources in order to test the theoretical model developed above.

III. EXPERIMENT

All light-soaking experiments described in this paper were performed on device quality undoped amorphous silicon deposited on Corning 7059 glass or on quartz substrates. Sample thicknesses varied between 1 and 1.6 μm. Defect densities were determined by standard subgap absorption spectroscopy using photothermal deflection and by electron spin resonance in the X-band (9.2 GHz, Bruker ER 300). Photoconductivity at room temperature was determined using coplanar contacts and

M. STUTZMANN, M. C. ROSSI, AND M. S. BRANDT

TABLE I. Characteristics of the different light sources used in this study: photon energy $(\hbar\omega)$, pulse duration (t_p), repetition rate $(\nu_{\rm rep})$, pulse energy density (E_p), pulse intensity (I_p), and average intensity $(\langle I\rangle)$.

Source	$\hbar\omega$ (eV)	t_p (s)	$\nu_{\rm rep}$ (s^{-1})	E_p (J cm^{-2})	I_p (W cm^{-2})	$\langle I\rangle$ (W cm^{-2})
Tungsten	$1-3$	cw				0.1
Kr$^+$	1.92	cw				0.3
Chopped Kr$^+$	1.92	3×10^{-4}	330	9×10^{-4}	3	0.3
Xe flash	$1-3$	2×10^{-6}	$30-300$	3×10^{-4}	160	$0.01-0.1$
Cu vapor	2.4	1×10^{-8}	7000	7×10^{-5}	7×10^3	0.5
CPM	2.0	1×10^{-13}	7000	4×10^{-5}	4×10^8	0.3

excitation with a HeNe-laser at 633 nm. The HeNe laser beam was defocused to achieve homogeneous illumination conditions. In addition, the active a-Si:H area was reduced to ≈ 2 mm $\times$ 1 mm when necessary to obtain homogeneous illumination conditions at high intensities. In some cases, also defocused light from a Kr$^+$ ion laser (647 nm) was used for photoconductivity measurements. Different light intensities were produced by inserting calibrated neutral density filters, i.e., without distorting intensity profiles.

Four different pulsed-light sources have been used, covering a broad range of pulse durations, t_p. Long light pulses have been produced by mechanical chopping of a high-intensity cw laser beam. Pulses in the microsecond time range were obtained from a high-intensity Xe flash lamp (Hamamatsu L 3071). Nanosecond light pulses with a high repetition rate were achieved using a Cu-vapor laser. Finally, femtosecond pulses were produced by a colliding-pulse mode-locked laser (CPM).[11] Further details of the pulsed-light sources are listed in Table I. In all cases, care was taken to limit the average light intensities and the individual pulse energy densities to a range where thermal effects are negligible.

IV. RESULTS AND DISCUSSION

A. Pulse illumination with monochromatic light sources

In order to obtain accurate information about the defect creation kinetics in a-Si:H it is essential to use monochromatic light sources with homogeneously absorbed light. In particular, there should be no significant gradient of the generation rate over a length scale given either by the (majority) carrier diffusion length or the sample thickness, whatever is larger. Otherwise, the different generation rates in different parts of the sample give rise to very complicated creation kinetics which can deviate quite significantly from the theoretical predictions of Sec. II. To illustrate this point, we show in Fig. 6 three light-induced degradation curves obtained by pulse illumination of the same sample with different wavelengths for the light-soaking source (λ_i) and for the probe beam used to monitor the photoconductivity decay (λ_p). The resulting degradation curves differ largely, depending on which particular combination of λ_i and λ_p

has been used. For $\lambda_i = 510$ nm and $\lambda_p = 633$ nm, almost no decrease of the photoconductivity is observed, because the degraded surface region of the sample has little influence on the secondary photocurrent excited by the weakly absorbed probe light. When both soaking and probing light are strongly absorbed $(\lambda_i = 510$ nm, $\lambda_p = 505$ nm), a much larger decrease of $\sigma_{\rm ph}(t)/\sigma_{\rm ph}(0)$ is observed for the same light-soaking treatment, since now approximately the same volume fraction is degraded and probed. However, note that the defect generation is governed by the np product, whereas $\sigma_{\rm ph}$ is determined mainly by n alone. Since holes have a much shorter diffusion length than electrons, for strongly absorbed photons there is still a spatial mismatch between the depth distribution of metastable dangling bonds and of photogenerated electrons, unless the sample is very thin. Experimental conditions suitable for an investigation of defect creation kinetics are only achieved for the third case shown in Fig. 6, where both light sources are weakly
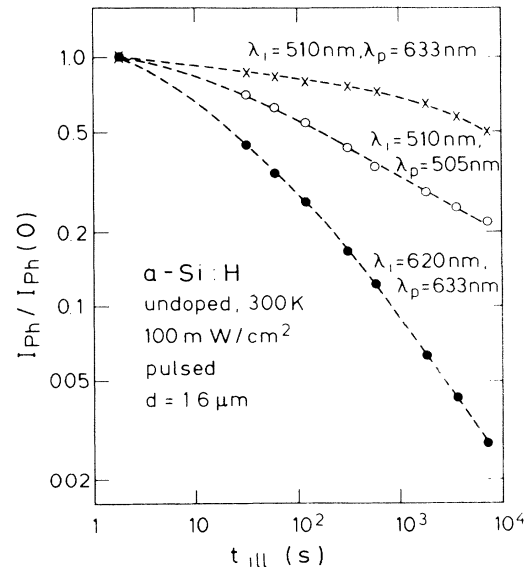

FIG. 6. Experimental results for the decrease of the normalized photocurrent $(I_{\rm ph}/I_{\rm ph}(0))$ in an a-Si:H sample (thickness 1.6 μm) during degradation with pulsed monochromatic light. Different curves correspond to different illumination (λ_i) and probing wavelengths (λ_p). Note the strong difference between degradation with strongly absorbed light $(\lambda_i = 510$ nm) and almost homogeneously absorbed light $(\lambda_i = 620$ nm) for otherwise identical experimental conditions.
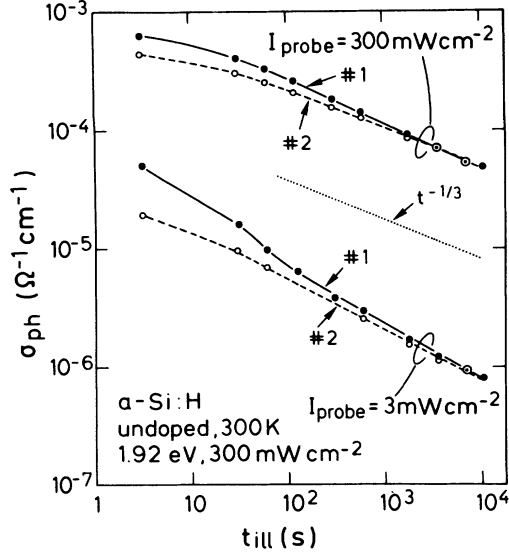
FIG. 7. Decay of the absolute photoconductivity, σ_{ph}, of the sample from Fig. 6 under constant illumination with monochromatic light ($h\nu = 1.92$ eV) with an intensity of 300 mW/cm². Different probing light intensities ($I_{probe} = 300$ mW/cm² and 3 mW/cm²) and to different experimental runs: 1 (solid) in the as-prepared state, 2 (dashed) after annealing at 200 °C for 1 h. The dotted line labeled $t^{-1/3}$ refers to the long-time decay expected from Eq. (3).
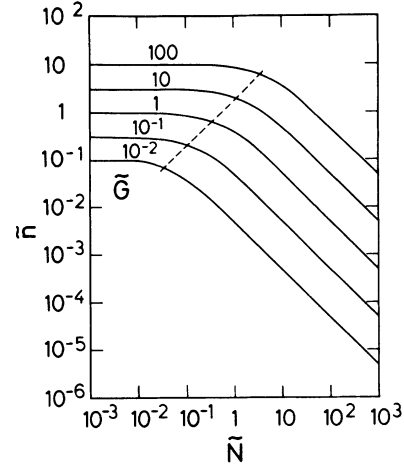

FIG. 8. Variation of the generalized free carrier density, $\tilde{n}$, on defect density, $\tilde{N}$, for different generation rates, $\tilde{G}$. The dashed line denotes the transition from bimolecular to monomolecular recombination.

absorbed ($\lambda_i = 620$ nm, $\lambda_p = 633$ nm). In this case, a decrease of σ_{ph} by almost two orders of magnitude is obtained in little more than 2 h using an average soaking intensity of only 100 mW/cm². The long-time slope of the decay is approximately $\sigma_{ph} \propto t^{-0.6}$, significantly faster than in the cw case, Fig. 4, with $I = 300$ mW/cm².

After these cautionary remarks, we now look in more detail at the defect creation by pulsed light compared to continuous illumination. For this comparison, we always use the same sample and keep the wavelengths of all light sources (pulsed or continuous) similar (620–647 nm). First, we show in Fig. 7 typical time dependencies of the photoconductivity during continuous illumination with an intensity of 300 mW/cm². The two sets of curves correspond to two different intensities which were used to monitor the photoconductivity (300 mW/cm², i.e., the same as the light-soaking intensity, and 3 mW/cm²). Curves labeled 1 and 2 were obtained starting from the as-deposited state and from an annealed state (180 °C, 1 h), respectively. The difference between these two starting conditions as far as the decay curves are concerned is most likely due to surface adsorbates, causing surface band bending. This increases the photoconductivity especially for low metastable defect densities (short illumination times) and low intensities of the probe light. In order to obtain the $t^{-1/3}$-time dependence expected in the long-time limit from Eq. (4), it is necessary to start from the annealed state where surface effects are much smaller. Then, we obtain a $t^{-0.33}$ time dependence for σ_{ph} probed with 300 mW/cm², whereas a somewhat stronger time

dependence of $t^{-0.44}$ is observed for low probing intensities. This variation of the kinetic exponent with probing intensity can be understood qualitatively on the basis of Fig. 8, where we show a plot of the generalized carrier density, $\tilde{n}$, versus the normalized defect density, $\tilde{N}$, with the normalized generation rate, $\tilde{G}$, as the curve parameter. Figure 8 is based on Eq. (1), similar to Figs. 1 and 2. Recall that a-Si:H in state A is characterized by $\tilde{N} = 1$, and that $\tilde{G} \approx 1$ corresponds to an illumination intensity of 100 mW/cm². Thus, for a probe light intensity of 3 mW/cm², we are clearly at all illumination times in the monomolecular limit of Eq. (1) ($\tilde{n} \propto \tilde{N}^{-1}$). For illumination and probing with 300 mW/cm², however, the transition from bimolecular to monomolecular recombination is only complete at $\tilde{N} \approx 10$ ($\overset{\triangle}{=} 10^{17}$ cm⁻³), so that for illumination times shorter than $\approx 10^4$ s the dependence of σ_{ph} on defect density in Fig. 7 will also be weaker.

In order to compare the results for continuous illumination described above with the case of pulse illumination, we have performed measurements of σ_{ph} under identical conditions (annealed starting state, 3 mW/cm² and 300 mW/cm² continuous probe intensities, $\hbar\omega \approx 2$ eV). The results obtained for two extreme pulse lengths are shown in Fig. 9. One source is a chopped high intensity laser light with a pulse width of 300 μs, a repetition rate of 330 Hz, and a pulse power of 1 W/cm². The second source is a colliding pulse laser with a pulse length of 100 fs, a repetition rate of 7 kHz, and a peak pulse power of 0.4 GW/cm². In both cases, the average power density on the sample is 300 mW/cm², as in the cw case. Also, the repetition rate is sufficiently low that complete electronic relaxation occurs between consecutive pulses. As can be seen from Fig. 9, the use of either pulse source leads to an acceleration of the photoconductivity degradation which, however, is much more pronounced for the shorter pulses. For a comparison of the experimental results with the theory developed above, we refer to Eqs.
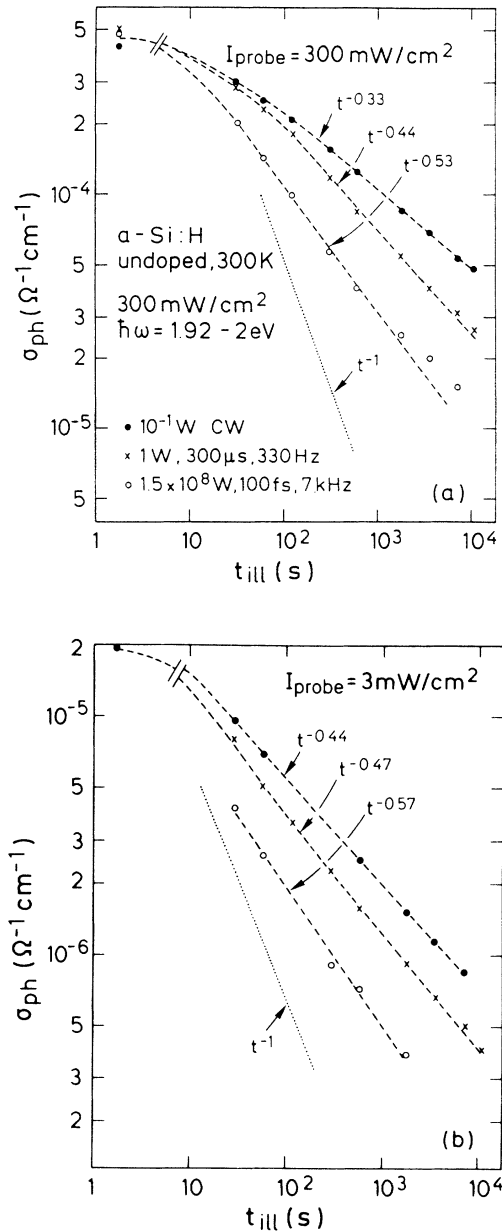
FIG. 9. Dependence of the photoconductivity on illumination time for the different (continuous or pulsed) light-soaking sources described in the text. In all degradation runs the average light intensity was 300 mW/ cm², and the incident photon energies were in the range 1.92–2 eV. (a) shows the decay of the photoconductivity monitored with a (cw) probing light intensity of 300 mW/cm², (b) shows similar results for a probe-light intensity of 3 mW/cm².

depend to some extent on the intensity of the probe light used to measure the photoconductivity. For high probe light intensities the acceleration factor of ≈ 8 is in good agreement with theory, but the time dependence changes from $t^{-0.33}$ to $t^{-0.44}$. For low probe light intensity, on the other hand, there is a good agreement for the asymptotic time dependence $(t^{-0.45})$, but the observed acceleration factor (≈ 4) is only half of what is expected. Nevertheless, we can conclude that the experimental results obtained with monochromatic pulse illumination are well accounted for by the general theory derived in Sec. II.

In addition to photoconductivity experiments we have also carried out electron spin resonance (ESR) measurements in order to test directly the increase in defect density giving rise to the photoconductivity degradation. A few ESR spectra comparing continuous and pulsed illumination are depicted in Fig. 10. In both cases a strong increase of the neutral dangling bond density is observed, which reaches $\approx 1 \times 10^{17} \text{cm}^{-3}$ after 4 h of irradiation with continuous light (cf. Fig. 4), but is as $6 \times 10^{17} \text{cm}^{-3}$ after only 2 h of light soaking with femtosecond pulses. This result agrees well with the photoconductivity data of Fig. 9(a), where we have found a conductivity ratio of about 4:1 for the two states of degradation shown in Fig. 10.

A remarkable result of our ESR measurements is that the defect density of $6 \times 10^{17} \text{cm}^{-3}$ observed in Fig. 10 is noticeably higher than the "saturated" metastable defect density of approximately $2 \times 10^{17} \text{cm}^{-3}$ obtained after very long cw irradiation. It has been argued in the liter-
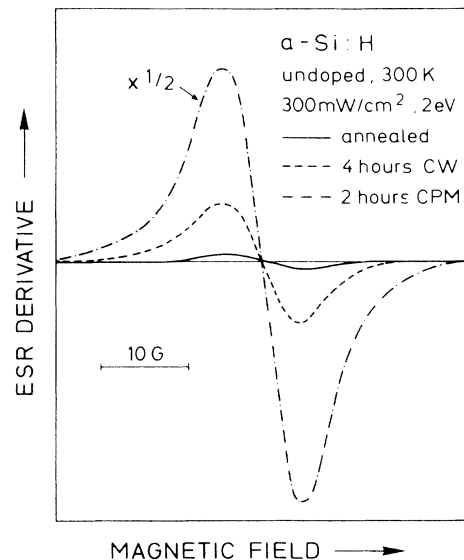
(12) and (18) for the femtosecond pulses, and to Eq. (26) for the long pulses. For the femtosecond pulses, we expect a variation of $\sigma_{ph} \propto t^{-0.5\cdots-0.7}$, which compares favorably with the experimental dependence $t^{-0.5\cdots-0.6}$. In the case of the long pulses we expect the same time dependence as for the cw illumination, and an acceleration approaching asymptotically a factor of $1/\eta = 10$ for the conditions chosen in Fig. 9. The experimental results

FIG. 10. Electron spin resonance (ESR) absorption derivative spectra for undoped a-Si:H at 300 K obtained in the annealed state (solid curve), after 4 h of continuous illumination with red light from a Kr^+-ion laser (300 mW/cm², dashed curve), and after 2 h of illumination with a pulsed colliding pulse mode-locked (CPM) laser of similar intensity and photon energy (dash-dotted curve). Note that for the latter case the ESR spectrum has been scaled down by a factor of two to fit in the same figure.

ature that this saturated value is caused by a limited density of defect creation sites which can transform under illumination into metastable dangling bonds.[6–8] It is clear from the three times higher defect density obtained after only 2 h of pulsed illumination that this simple model is not correct. (In fact, even higher spin densities will be shown in the next section.) Triggered by the results in Fig. 10, we have studied the origin of an apparent defect saturation for continuous illumination in more detail. We have found that the saturation is indeed a steady state between light-induced metastable defect creation on one side, and thermal as well as light-induced annealing of defects on the other side. The interested reader is referred to Ref. 13 for more information on this topic.

Following our earlier report on degradation of amorphous silicon by short-light pulses,[2] various other groups have studied this effect also using different light sources such as frequency-doubled YAG lasers, dye lasers, ruby lasers, etc. In most of these investigations a fast saturation of metastable defects was observed, however, at more elevated levels ($\approx 5 \times 10^{17} \, \text{cm}^{-3}$ versus $\approx 2 \times 10^{17} \, \text{cm}^{-3}$ for cw), contrary to our findings.[14,15] A common criticism to these investigations is that pulses with too high energies ($E_p \geq 10 \, \text{mJ/cm}^2$) were employed causing a considerable heating during the pulse. This heating will give rise to a non-negligible annealing rate, thus providing an explanation for the observed saturation. We have measured the temperature rise in a-Si:H during an intense pulse with the help of a thin-film a-Ge:H thermometer[16] and find the experimental results in good agreement with our simple estimate in Eq. (5). As a rule of thumb, pulse heating of a-Si:H can no longer be neglected for pulse energies larger than $2 \, \text{mJ/cm}^2$. A theoretical approach to incorporate light-induced annealing into the defect-creation kinetics for pulsed light-soaking has recently been published by Meaudre $et \, al.$[17]

From a more practical point of view, an interesting question is at what levels of metastable dangling bond defect densities the degradation process of undoped amorphous hydrogenated silicon may eventually saturate, if at all. In cw experiments, saturation densities below $2 \times 10^{17} \, \text{cm}^{-3}$ are usually reported[14] (and references therein). In our pulsed light-soaking experiments performed with low power lasers or flash lamps, defect densities up to $10^{18} \, \text{cm}^{-3}$ are routinely achieved, however, after relatively long irradiation times of several hours. More recently we have used a Nd-YAG pumped optical parametric oscillator (OPO) operating around 700 nm with a pulse energy of several 10 mJ and a repetition frequency of 30 Hz to establish a useful lower limit for the saturated metastable defect density of a-Si:H. The main advantage of OPO's over other pulsed-light sources is that the tuneability allows to achieve optimal homogeneous absorption throughout a typical a-Si:H sample of thickness $\approx$ 1–2 μm. Within less than 30 min of irradiation with this homogeneously absorbed light source (pulse length $\leq$ 10 nsec), a reversible increase of the defect density in a-Si:H to more than $3 \times 10^{18} \, \text{cm}^{-3}$ could be achieved. Thus, there appears to be no technologically interesting upper bound for metastable defects in a-Si:H, e.g., because of structural reasons such as impurity con-

centrations. Instead, metastable defect densities achievable by suitable pulse illumination are now comparable with typical defect densities ($\approx 10^{19} \, \text{cm}^{-3}$) observed after irradiation of a-Si:H with energetic particles.

B. White light pulse illumination

We have mentioned in the introduction that pulse irradiation may also provide an interesting method for accelerated stability tests of amorphous Si solar cells.[4,16] For this purpose it is desirable to use pulsed-light sources with a spectrum of emitted photon energies as close to the solar AM1 or AM1.5 spectra as possible. We have found that Xe flash lamps with a suitable filter arrangement are a very attractive, low-cost alternative to pulsed lasers. In this section, therefore, we will present a detailed investigation of degradation of a-Si:H using Xe flash lamps. The relevant parameters of the particular flash lamp used in our experiments have already been presented in Table I. With a pulse duration of $t_p \approx 2 \, \mu$sec, one is essentially operating in the limit of quasicontinuous illumination leading to a kinetic behavior described by Eqs. (26) or (27). Due to the polychromatic light, however, a simple kinetic behavior is not expected, as already discussed in the context of Fig. 6. We will instead put more emphasis on the effects of variation of the repetition frequency and pulse length on the degradation of a-Si:H.

To begin, we show in Fig. 11 a comparison between the photoconductivity degradation due to illumination with continuous white light and pulsed light, respectively, with an average intensity of $100 \, \text{mW/cm}^2$ in both cases. Using suitable cutoff filters, the spectral intensity distribution of the cw light source and the Xe-flash lamp can be made sufficiently similar so that the differences seen in Fig. 11 are mainly caused by the different time distribution of the incoming photons. As in the case of monochromatic light sources, a strong acceleration of the degradation is observed upon pulsed irradiation (about two orders of magnitude for long illumination times). As is evident from the comparison of Figs. 11(a) and 11(b), the decrease of σ_{ph} is almost identical for optically thin ($d = 0.5 \, \mu$m) and thick samples ($d = 2.5 \, \mu$m), except for an initially higher photoconductivity in the thicker sample. Note that σ_{ph} was monitored with the same monochromatic source (HeNe laser, $\hbar\omega = 1.92$ eV, $50 \, \text{mW/cm}^2$) as for the case of monochromatic light soaking in the previous section. The main difference between the kinetic behavior seen for polychromatic versus monochromatic light soaking is a weaker asymptotic time dependence for the former ($t^{-0.25} - t^{-0.33}$, instead of $t^{-0.33} - t^{-0.6}$ in Fig. 9). This is in accordance with Fig. 6, noting that most of the photons of a white light source are either strongly absorbed ($\alpha d \gg 1$) or else not absorbed ($\alpha d \ll 1$).

For the thin sample in Fig. 11(a), we expect the photoconductivity to be a good measure of the average defect density, since the sample thickness is comparable to the electron diffusion length. Indeed, a comparison of σ_{ph} and the dangling bond defect density N_S obtained from ESR on the same sample exhibits the inverse rela-
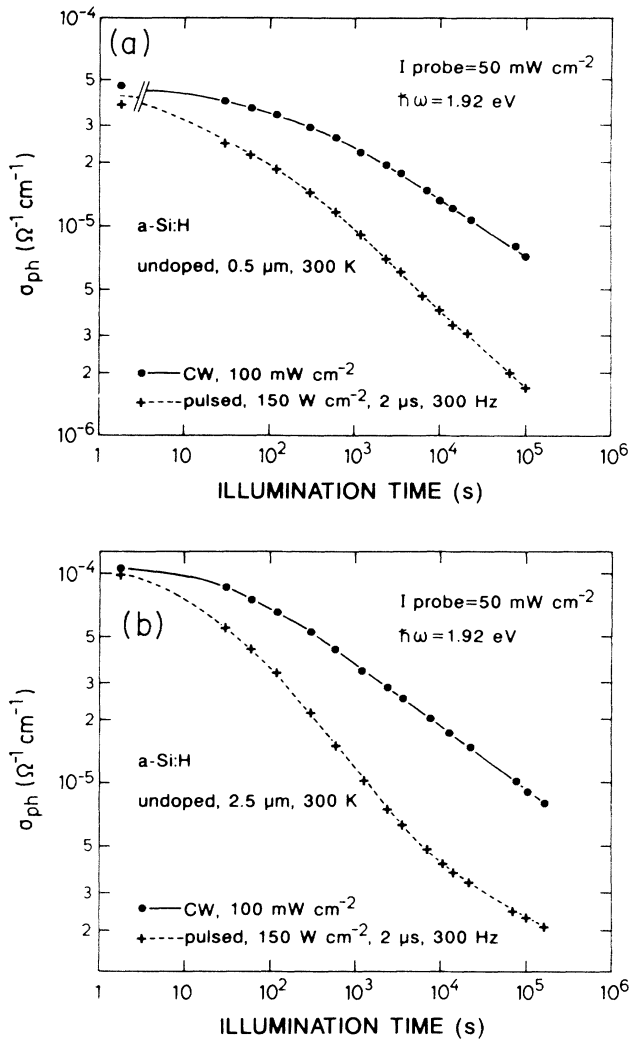
FIG. 12. Correlation between the ESR defect density (N_S) and the inverse photoconductivity (σ_{ph}^{-1}) for a thin a-Si:H sample subjected to pulsed light soaking with a Xe flash lamp.

FIG. 11. Comparison of photoconductivity fatigue curves for continuous (cw) and pulsed illumination with white light of average intensity 100 mW/cm^2 (a) sample thickness (0.5 μm) comparable to electron drift length; (b) sample thickness (2.5 μm) much larger than electron drift length. The photoconductivity in both cases has been monitored by defocused cw laser light (50 mW/cm^2, $\hbar\omega = 1.92$ eV).

rithm of the illumination time, in order to allow a better comparison with the cw-photoconductivity data in Fig. 11. With increasing defect density, we observe a decrease of the peak current by a factor of two, together with a corresponding decrease of the decay time. (Note that the decay time of the photon pulse itself is about 1–2 μs so that the current decay time is at least as long as this value.) The observation that the induced current pulse is essentially independent of the metastable defect density is in accordance with the general relation Eq. (1) as depicted in Fig. 1: the peak light intensity during a pulse of our flash lamp is about 150 W/cm^2, correspond-

tion $\sigma_{ph} \propto N_S^{-1}$ expected for monomolecular recombination (Fig. 12). Therefore, for thin layers we can relate the photoconductivity results directly to our theory of metastable defect creation by pulsed irradiation also in the case of polychromatic irradiation.

An interesting question which can be addressed experimentally using the relatively long light pulses of the Xe flash lamp concerns the temporal distribution of the transient carrier density during and after the pulse as a function of illumination time. Typical results obtained for the 0.5 μm thick sample are shown in Figs. 13 and 14. Figure 13 summarizes the actual current transients as a function of illumination time (solid curves) compared to the optical pulse itself (dashed curve). In Fig. 14 the peak currents and characteristic current decay times deduced from these curves are plotted against the loga-
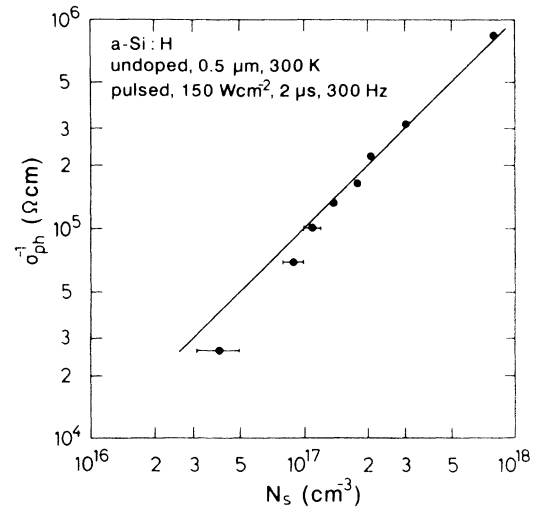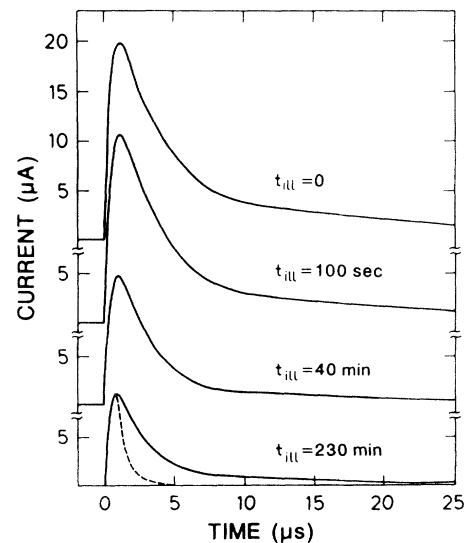

FIG. 13. Photocurrent transients of the thin a-Si:H sample ($d = 0.5$ μm) described already in Figs. 11(a) and 12 after different illumination times with the Xe flash lamp. The dashed curve shows the time variation of the flash-lamp light intensity during a single pulse.
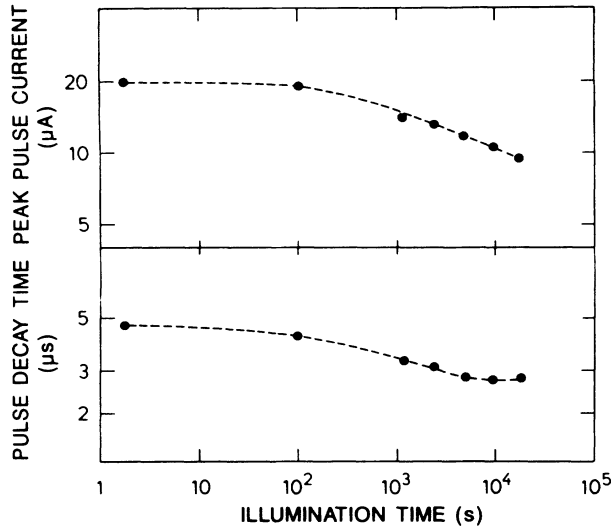
FIG. 14. Peak pulse current and average pulse decay time of the current transients shown in Fig. 13 as a function of illumination time.
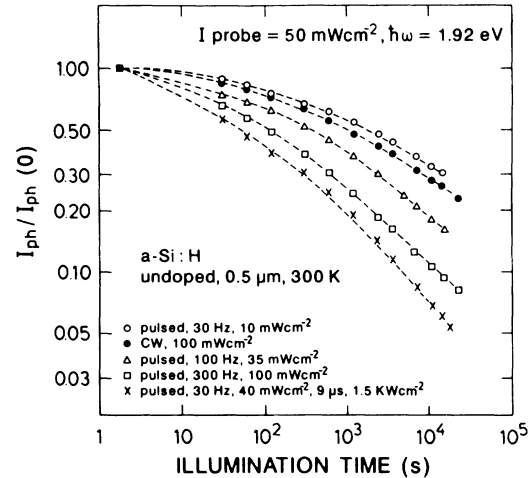

FIG. 15. Normalized photoconductivity decay curves for different light-soaking conditions using either constant white-light illumination, or flash-lamp treatment with different repetition rates or pulse lengths. (Thin sample, probed with 50 mW/cm^2 at 1.92 eV.)

ing to a generalized generation rate of $\bar{G} \approx 10^3$ in Fig. 1. For this generation rate, a factor of two decrease in carrier density $\bar{n}$ requires an increase of the defect density from 10^{16} cm^{-3} to about 3×10^{17} cm^{-3}, which is in excellent agreement with the σ_{ph} and N_S data in Figs. 11(a) and 12. From Fig. 1 we can further conclude that carrier recombination during the intense pulse remains essentially bimolecular, explaining the weak dependence of the average pulse decay time on illumination time.

One advantage of using a flash lamp for pulse degradation is that it is relatively easy to change the repetition rate ν_{rep} and also the pulse duration t_p. We expect from Eq. (26) that this should have a well defined effect on the rate of defect creation which should essentially be given by the duty cycle $\eta = \nu_{rep}t_p$, at least to the extent that the long-pulse limit $(t_p \gg \tau)$ is valid. Experimental results for different values of ν_{rep} and t_p are summarized in Fig. 15, again with the cw illumination case shown for comparison. In three of the curves shown in Fig. 15 only the repetition rate has been changed so that the average intensity $\langle I \rangle = E_p\nu_{rep}$ changes accordingly. From Eq. (26) we expect that the only effect of a change in ν_{rep} is a corresponding change in the illumination time required to obtain a given degradation. By plotting the photoconductivity as a function of $\nu_{rep} \times t_{ill}$ (i.e., as a function of the total number of pulses applied to the sample), all degradation curves should coincide. As shown in Fig. 16, this is indeed the case to a very good approximation. Small deviations only occur for the lowest repetition rate of 30 Hz and are probably mainly due to a frequency dependence of the flash lamp pulse shape. In particular, we can conclude from the data in Fig. 16 that thermal effects can be neglected in our pulse-light experiments. An important observation in Fig. 15 is that the degradation caused by cw illumination with 100 mW/cm^2 can be reproduced quite accurately with a repetition rate of 30 Hz, for which the average intensity is an order of mag-

nitude lower, 10 mW/cm^2. This allows us to conclude that the state of degradation induced by our white-light flashes is indeed quite similar to the cw case as far as its macroscopic consequences for photoconductivity are concerned. Thus, the simple scaling proportional to ν_{rep} in Fig. 16 can be used to develop an accelerated degradation test for a-Si:H films and devices with a well-defined acceleration factor. Further details concerning this application of pulsed light soaking are described in Refs. 4 and 16.

A question of more fundamental importance is how the experimental results in Fig. 15 relate to the predictions of the theory outlined in the first part of this paper. Since the pulse durations of the order of μs produced by Xe flash lamps actually fall between the short and long pulse limits, $t_p \ll \tau$ and $t_p \gg \tau$ discussed above, and also deviate significantly from the assumed temporal distribu-
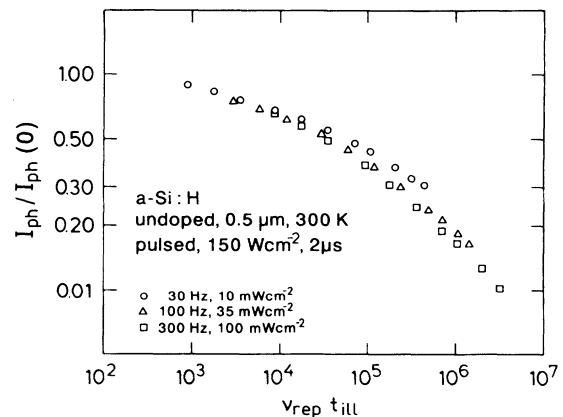

FIG. 16. Normalized photoconductivity decays as a function of pulse count $(\nu_{rep} \times t_{ill})$ from Fig. 15 (for 2 μs pulse length).

TABLE II. Experimental and theoretical acceleration factors for pulsed light soaking of amorphous silicon with white light. The acceleration factor is defined as the ratio of the light-soaking times required to reach a conductivity degradation by a factor of three for pulsed illumination versus cw-illumination (cf. Fig. 15). Equation (26) refers to the long-pulse limit ($t_p \gg \tau$), Eq. (18) to the short-pulse limit ($t_p \ll \tau$) in the theoretical derivation. Monomolecular photoconductivity ($\tau_{ph} \propto 1/N$) has been assumed for the comparison. (* indicates a normalized value.)

Conditions			Acceleration factors		
ν_{rep} (s^{-1})	t_p (μs)	$\langle I \rangle$ (mW/cm^2)	Eq. (26)	Eq. (18)	exp.
cw		100	1		1
30	2	10	5.5	1*	0.6
100	2	35	8.5	4	3.5
300	2	100	12	8.3	14
30	9	40	8.5	4.3	24

tion of a square pulse (cf. Fig. 13), an exact quantitative discussion would require a numerical solution of Eq. (5) and the ensuing expression for $N(t)$. In addition, the use of a white light source would require a more complicated model accounting for the spatially inhomogeneous generation rate profile within a thin film of a-Si:H.

Nevertheless, a semiquantitative comparison can be made between the results in Fig. 15 and Eqs. (18) or (26), which describe the limiting cases of short and long pulses, respectively. As shown in Table II, the short-pulse limit, Eq. (18) is still a good approximation for $t_p = 2$ μs. In particular, the strong, almost linear dependence of the speed of degradation on repetition rate ν_{rep} is well reproduced. An absolute comparison between theory and experiment is not possible, since Eq. (18) contains unknown proportionality factors which cannot be determined by matching to the cw case. For $t_p = 9$ μs, the short-pulse approximation obviously is no longer valid, theory and experiment differ by almost an order of magnitude. Using the long-pulse approximation, Eq. (26), on the other hand, the experimentally observed acceleration of about a factor of ten for $\langle I \rangle = 100$ mW/cm^2 is well reproduced, but the acceleration factor is almost insensitive to changes in ν_{rep} and t_p, in contrast to the experimental findings. Obviously, the microsecond pulses produced by the Xe flash lamp fall right between the extreme cases $t_p \ll \tau$ and $t_p \gg \tau$, for which closed theoretical expressions could still be derived.

Not reproduced by the theory is the strong dependence of light-induced changes on the pulse length for equal average intensity ($t_p = 2$ μs or $t_p = 9$ μs, $\langle I \rangle \approx 40$ mW in Table II and Fig. 15). The most likely reason for this discrepancy is the strong deviation of the pulse produced by the flash lamp from the square pulse assumed in the theory. A quantitative investigation of this question again would require numerical simulation and will not be justified for white light illumination because of other constraints of white light illumination mentioned earlier.

V. SUMMARY AND CONCLUSIONS

The aim of the present investigation has been to investigate the influence of pulsed-light illumination on

the degradation behavior (Staebler-Wronski effect) in undoped hydrogenated amorphous silicon. Based on the weak-bond dangling bond conversion process due to nonradiative recombination of localized electron-hole pairs (excitons), a detailed theory for the kinetics of metastable dangling bond creation was derived, which describes the influence of pulse parameters (repetition rate, pulse duration, average intensity) on the degradation process. The theory predicts a strong acceleration of defect formation during pulse illumination, which is due to the nonlinear dependence of the defect creation rate on carrier density: $dN/dt \propto n \times p \approx n^2$. Because of this nonlinearity, defect formation proceeds more effectively when the same number of photons are bunched in short, intense pulses rather than impinging in a low, continuous flux. Specific kinetic expressions for the limiting cases of short pulses ($t_p \ll \tau$, where τ is the carrier recombination time constant) and long pulses ($t_p \gg \tau$) can be derived analytically under reasonable simplifying assumptions.

Experiments with different pulsed-light sources (femtosecond lasers, Cu vapor laser, chopped cw lasers, flash lamps) have been performed on state-of-the-art undoped a-Si:H films, in order to test these theoretical predictions. We generally observe a good quantitative agreement between theory and experiment, notably a strong acceleration of metastable dangling bond creation in a-Si:H by up to two orders of magnitude in illumination time for short-pulse light soaking compared to cw illumination with the same average intensity. Using such accelerated aging methods, metastable defect densities in excess of 10^{18} cm^{-3} have been produced in device quality a-Si:H, thus invalidating the concept of a unique saturated metastable defect of about 2×10^{17} cm^{-3} used in other theories.

We would like to close with a few general remarks concerning the implications of pulsed-light-soaking experiments for other theories of light-induced metastability in a-Si:H. At present, basically four different kinds of theories exist.

(i) Defect creation by excitonic recombination as used throughout this paper.

(ii) Trapping of photoexcited carriers at charged defects involving a distribution of barriers.[18]

(iii) Stretched-exponential relaxation, e.g., due to light-induced dispersive hydrogen motion.[7,19]

(iv) Partial thermal equilibration between defects and tail states as a function of quasi-Fermi level position.[20]

As it stands, only the bimolecular recombination model can *ad hoc* be easily reconciled with the strong enhancement of metastable defect production upon pulsed light soaking. Models involving linear dependencies of metastable defect formation on carrier density or the explicit time dependence in stretched-exponential relaxation, on the other hand, will need to be reconsidered in view of the present results.

Moreover, a complete description of metastable defect creation and annealing has to go far beyond the already complicated theoretical description outlined in the present paper. As discussed in detail by Bube and Redfield,[21] creation and annealing of metastable defects may, in principle, occur both via light-induced and purely thermal processes. Indeed, all four resulting basic processes (light-induced creation, thermal creation, light-induced annealing, thermal annealing) have been described in the literature and, in general, have to be included into a complete picture. However, in practice simplifications are possible because light-induced creation and thermal annealing usually dominate thermal creation and light-induced annealing. Particularly, in the early stages of pulsed light soaking only light-induced defect creation has to be considered as the dominant term. This simplification has been used throughout the present paper. A more complete description which also should involve distributions of defect creation and annealing rates because of structural disorder, remains a challenge for future work. First steps into this direction have been attempted by Meaudre *et al.*,[17] who include light-induced annealing into their rate equations for pulse soaking of *a*-Si:H. In this sense, the variability of pulsed light-soaking conditions will eventually provide better experimental tests for existing theories than standard cw light soaking.

ACKNOWLEDGMENTS

* Permanent address: Walter Schottky Institut, Technische Universität München, Am Coulombwall, D-85748 Garching, Germany.

[1] M.S. Brandt and M. Stutzmann, J. Appl. Phys. **75**, 2507 (1994).

[2] M. Stutzmann, J. Nunnenkamp, M.S. Brandt, and A. Asano, Phys. Rev. Lett. **67**, 2347 (1991).

[3] M. Stutzmann, J. Nunnenkamp, M.S. Brandt, A. Asano, and M.C. Rossi, J. Non-Cryst. Solids **137&138**, 231 (1991).

[4] M.C. Rossi, M.S. Brandt, and M. Stutzmann, Appl. Phys. Lett. **60**, 1709 (1992).

[5] M. Stutzmann, W.B. Jackson, and C.C. Tsai, Phys. Rev. B **32**, 23 (1985).

[6] M. Cutrera, R.R. Koropecki, A.M. Gennaro, and R. Arce, Phys. Rev. B **35**, 1442 (1987).

[7] D. Redfield and R.H. Bube, Appl. Phys. Lett. **54**, 1037 (1989).

[8] H.R. Park, J.Z. Liu, and S. Wagner, Appl. Phys. Lett. **55**, 2658 (1989).

[9] U. Schneider, B. Schröder, and F. Finger, J. Non-Cryst. Solids **97&98**, 795 (1987).

[10] S. Scholz and B. Schröder, J. Non-Cryst. Solids **137&138**, 259 (1991).

[11] J. Feldmann, J. Nunnenkamp, G. Peter, E. Göbel, J. Kuhl, K. Ploog, P. Dawson, and C.T. Foxon, Phys. Rev. B **42**, 5809 (1990).

[12] According to results obtained from spin-dependent photoconductivity [H. Dersch *et al.*, Phys. Rev. B **28**, 4678 (1983)], the main channel for recombination via defects in undoped *a*-Si:H is capture of an electron by a neutral dangling bond, followed by capture of a hole by the resulting negatively charged defect. Both transition probabilities are indeed quite similar, about $2 \times 10^{-9} \, \text{cm}^3 \, \text{s}^{-1}$ (Ref. 5).

[13] C.F.O. Graeff, R. Buhleier, and M. Stutzmann, Appl. Phys. Lett. **62**, 3001 (1993).

[14] N. Hata, G. Ganguly, S. Wagner, and A. Matsuda, Appl. Phys. Lett. **61**, 1817 (1992).

[15] J. Kocka, O. Stika, and O. Klima, Appl. Phys. Lett. **62**, 1082 (1993).

[16] M. Stutzmann, C.F.O. Graeff, M.C. Rossi, and M.S. Brandt, Braz. J. Phys. **23**, 124 (1993).

[17] R. Meaudre, S. Vignoli, M. Meaudre, and L. Chanel, Philos. Mag. Lett. **68**, 159 (1993).

[18] R.S. Crandell, Phys. Rev. B **43**, 4057 (1991).

[19] J. Kaklios, R.A. Street, and W.B. Jackson, Phys. Rev. Lett. **59**, 1037 (1987).

[20] P.V. Santos and W.B. Jackson, J. Non-Cryst. Solids **137&138**, 203 (1991).

[21] R.H. Bube and D. Redfield, J. Appl. Phys. **66**, 820 (1989).